Differential Scanning Calorimetry Study of the Thermodynamic Stability of Some Mutants of Sso7d from *Sulfolobus solfataricus*†

Francesca Catanzano,‡ Giuseppe Graziano,§ Paola Fusi,|| Paolo Tortora,|| and Guido Barone*,‡

Dipartimento di Chimica, Università di Napoli "Federico II", Via Mezzocannone, 4, 80134 Napoli, Italy, Facoltà di Scienze, Università del Sannio, Via Marmorale, 82020 Paduli (BN), Italy, and Dipartimento di Fisiologia e Biochimica Generali, Università di Milano, Via Celoria, 26, 20133 Milano, Italy

Received December 4, 1997; Revised Manuscript Received May 4, 1998

ABSTRACT: Sso7d from the thermoacidophilic archaebacterium *Sulfolobus solfataricus* is a small globular protein with a known three-dimensional structure. Inspection of the structure reveals that Phe31 is a member of the aromatic cluster forming the protein hydrophobic core, whereas Trp23 is located on the protein surface and its side chain exposed to the solvent. The thermodynamic consequences of the substitution of these two residues in Sso7d have been investigated by comparing the temperature-induced denaturation of Sso7d with that of three mutants: F31A-Sso7d, F31Y-Sso7d, and W23A-Sso7d. The denaturation processes proved to be reversible for all proteins, and represented well by the two-state N ⇔ D transition model in a wide range of pH. All three mutants are less thermally stable than the parent protein; in particular, in the pH range of 5.0−7.0, the F31A substitution leads to a decrease of 24 °C in the denaturation temperature, the F31Y substitution to a decrease of 10 °C, and the W23A substitution to a decrease of 6 °C. A careful thermodynamic analysis of such experimental data is carried out.

The physicochemical rationalization of the relationship between a given tertiary structure and its thermodynamic stability has attracted much interest in recent years. Such research is closely related to the classic problem of protein folding, since Anfinsen (*1*) demonstrated that this fundamental process is ruled by the "thermodynamic hypothesis". All the experimental investigations performed so far have pointed out that the native structure of globular proteins from mesophilic organisms possesses only marginal stability (*2*). However, thermophilic microorganisms are able to live under extreme temperature conditions; the upper temperature limit of viability seems to be approximately 150 °C (*3*). As microorganisms are isothermal in their habitat, they cannot avoid the thermal stress and must adapt their biological functions to the extreme temperature. In fact, proteins extracted from thermophilic microorganisms are still fully active at temperatures near or above the boiling point of water. Thermophilic proteins are made up of the same 20 natural amino acids, and the stability of the native conformation is ensured by the same noncovalent interactions that are operating in mesophilic proteins. It is hard to try to understand how the balance among stabilizing and destabilizing factors has been optimized during evolution to cope with such high temperatures (*4*).

A thermodynamic study of the extrastability of thermophilic proteins requires a quantitative determination of the changes in the state functions associated with the denaturation process, $\Delta_d G$, $\Delta_d H$, $\Delta_d S$, and $\Delta_d C_p$. The best approach for performing such a task is provided by differential scanning calorimetry (DSC)[1] which allows the direct evaluation of the denaturation enthalpy and heat capacity changes, and, provided that the process is a reversible two-state transition, allows the calculation of the Gibbs energy and entropy changes.

Sso7d has been recently isolated from *Sulfolobus solfataricus* (*5, 6*), a thermoacidophilic archaebacterium that lives at 87 °C and acidic pH in volcanic hot springs (*7*). Formerly, we referred to this molecule as P2 (*6*); however, on the basis of amino acid sequence, P2 and Sso7d were proven to be the same molecule. We have subsequently cloned the protein-encoding gene and expressed it in *Escherichia coli* (*8*). The recombinant protein was identical to the natural form, the only difference being the absence of monomethylation at Lys4 and Lys6. Sso7d is a small basic ($pI = 10.2$), 63-residue protein that contains no histidine or asparagine, and no cysteine. The physiological role of the protein is not clear yet; it is able to bind DNA nonspecifically, thus protecting DNA from thermal denaturation (*9, 10*), but also has a ribonuclease activity (*6*). Its tertiary structure in solution, determined by NMR (*11, 12*), shows that the protein is folded into a compact globular unit composed of a three-stranded antiparallel β-sheet which is orthogonal to a two-

† Work supported by a PRIN grant from the Italian Ministry for University and Scientific and Technological Research (MURST, Rome) and funds from the Italian National Research Council (CNR, Rome).

* To whom correspondence should be addressed. Fax: +39/81/5527771. E-mail: barone@chemna.dichi.unina.it.

‡ Università di Napoli "Federico II".

§ Università del Sannio.

|| Università di Milano.

[1] Abbreviations: Sso7d, 7 kDa DNA-binding protein from *Sulfolobus solfataricus*; F31A-Sso7d and F31Y-Sso7d, mutants of Sso7d where phenylalanine 31 is replaced by alanine and tyrosine, respectively; W23A-Sso7d, mutant of Sso7d where tryptophan 23 is replaced by alanine; CD, circular dichroism; DSC, differential scanning calorimetry; ASA, accessible surface area; NMR, nuclear magnetic resonance; FTIR, Fourier transform infrared spectroscopy; SDS−PAGE, sodium dodecyl sulfate−polyacrylamide gel electrophoresis.

S0006-2960(97)02994-2 CCC: $15.00
Published on Web 06/27/1998

stranded antiparallel β-sheet, and with only a small helical stretch at the C terminus. Sso7d has a hydrophilic surface with many basic residues (i.e., 2 arginines and 14 lysines) and a very hydrophobic core with a cluster of aromatic side chains (Phe5, Tyr7, Phe31, and Tyr33) with herringbone geometry. Its small size allowed us to construct and express, with relative ease, several mutant forms. Therefore, Sso7d is a suitable tool for investigating the thermodynamic stability of thermophilic proteins and for clarifying its origin at a molecular level. In fact, Ladenstein and co-workers (*13*) reported a comprehensive and detailed study on the temperature-induced denaturation of Sso7d performed by means of CD and DSC measurements. The process proved to be reversible and represented well by the two-state N ⇔ D transition model.

In this paper, we report on the thermodynamic characterization of three mutants of Sso7d: F31A-Sso7d, F31Y-Sso7d, and W23A-Sso7d. The sites of amino acid substitutions were suitably selected in order to bring out the structural determinants of protein thermal stability. Indeed, Phe31 is a member of the aromatic cluster in the protein core which is considered fundamental for the stability of the native conformation. In contrast, Trp23 is located on the protein surface, and its side chain seems to play a major role in the DNA binding process (*9*). We carried out DSC measurements in a wide range of pH and performed a careful analysis of experimental data. It is shown that all three mutants are less thermally stable than the parent protein; in the pH range of 5.0−7.0, the F31A substitution causes a decrease of 24 °C in the denaturation temperature, the F31Y substitution a decrease of 10 °C, and the W23A substitution a decrease of 6 °C. These findings are discussed, and a tentative explanation is proposed.

MATERIALS AND METHODS

Sso7d from the archaebacterium *S. solfataricus* was expressed in *E. coli* and purified as described (*8*). The recombinant protein was indistinguishable from the wild-type Sso7d (*8*). The F31A, F31Y, and W23A mutants were obtained by site-directed mutagenesis as reported (*14*). The purity of the four proteins was confirmed by means of SDS−PAGE. The enzymes were lyophilized after exhaustive dialysis against MilliQ water, stored at −20 °C, and dissolved just before use in the buffer. Under these conditions, the enzymes were indefinitely stable. Before DSC measurements, sample solutions were dialyzed against the required buffer at 4 °C for 24 h and degassed for 5 min. Dialysis tubes with a cutoff limit of 3500 Da were used.

The protein concentration of dialyzed samples was determined spectrophotometrically using extinction coefficients calculated by the method of Gill and von Hippel (*15*) from the absorption of tyrosine (ϵ_{280} = 1400 M^{-1} cm^{-1}) and tryptophan (ϵ_{280} = 5500 M^{-1} cm^{-1}).

Buffers purchased from Sigma included glycine HCl for pH 2.3−3.6, acetic acid/sodium acetate for pH 3.8−5.2, and MES [2-(*N*-morpholino)ethanesulfonic acid] for pH 5.5−7.2. All the solutions contained 10 mM buffer and 100 mM NaCl. The buffers employed have low protonation enthalpies (*16*), and therefore, the pH depends little on temperature. Doubly deionized water was used throughout. The pH of all samples was measured before each DSC measurement, at 25 °C, with a Radiometer pHmeter (model PHM93).

Scanning Calorimetry. Calorimetric measurements were carried out on a Setaram Micro-DSC apparatus, able to work in the temperature range of 0−100 °C, and interfaced with a data translation A/D board for automatic data accumulation. A scan rate of 1.0 K min^{-1} was chosen for this study, and the data were recorded every 1 s. All data analyses were carried out with software developed in our laboratory (*17*). The raw data were converted to an apparent molar heat capacity (kilojoules per kelvin per mole), by correcting for the instrument calibration curve and the buffer−buffer scanning curve, and dividing each data point by the scan rate and the number of moles of protein in the sample cell. Finally, the apparent molar heat capacity was converted to the excess molar heat capacity, $\langle \Delta C_p \rangle$, assuming that the native state heat capacity was as the reference baseline (*18*, *19*). For a reliable evaluation of such a baseline by linear regression on the pretransition region, DSC scans always started from 5 °C.

Due to the small size of Sso7d, the overall molar heat effect of denaturation is not large; i.e., the DSC peaks are small and broad, which complicates an accurate evaluation of the thermodynamic parameters. To obtain reliable records of the heat capacity profiles, we had to work at relatively high protein concentrations (2.5−5.5 mg mL^{-1}); nevertheless, neither the concentration nor the heating rate dependence (in the range of 0.5−1.5 K min^{-1}) of the heat capacity peaks was observed. Moreover, the DSC peaks extend beyond 100 °C in most of the experiments, due to the high denaturation temperature and low denaturation enthalpy change of the proteins investigated. Therefore, our instrument recorded incomplete DSC peaks, and an analysis different from the conventional one had to be carried out.

Analysis of DSC Data. The excess molar heat capacity function for a two-state N ⇔ D transition has the following form (*18*−*20*):

$$\langle \Delta C_p(T) \rangle = [\Delta_d H(T_d) + \Delta_d C_p(T - T_d)](df_D/dT) + f_D \Delta_d C_p \quad (1)$$

where f_D equals $[K_d/(1 + K_d)]$ and is the fraction of denatured molecules and K_d is the corresponding equilibrium constant, whose temperature dependence is given by

$$K_d = \exp -\{[\Delta_d H(T_d)/R][(1/T) - (1/T_d)] + (\Delta_d C_p/R)[1 - (T_d/T) - \ln(T/T_d)]\} \quad (2)$$

where $K_d = 1$ for $T = T_d$, the denaturation temperature, and $\Delta_d H(T_d)$ and $\Delta_d C_p$ represent the denaturation enthalpy and heat capacity changes, respectively. Equation 2 is correct in the assumption that $\Delta_d C_p$ is temperature-independent.

The first term on the right-hand side of eq 1 gives rise to the bell-shaped curve characteristic of DSC transitions, whereas the second term represents the shift in baseline resulting from the difference in heat capacity between the denatured and native states of the protein (i.e., the heat capacity change is distributed over the temperature range where the denaturation occurs, in proportion to the advancement degree of the process). Equation 1 is an analytical relationship that allows the calculation of simulated two-state DSC profiles, using as input parameters the values of T_d, $\Delta_d H(T_d)$, and $\Delta_d C_p$. By performance of a nonlinear regression of the experimental DSC profiles with respect to

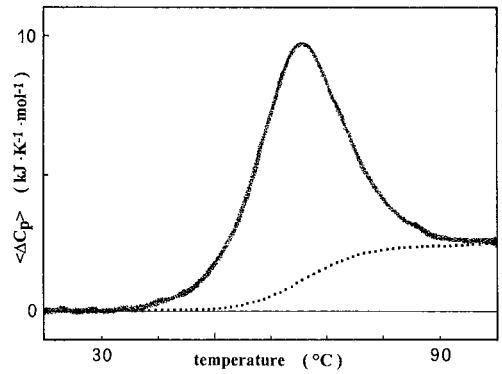

FIGURE 1: DSC profile of Sso7d at pH 2.5 with 10 mM glycine HCl buffer and 100 mM NaCl and a protein concentration of 3.2 mg mL^{-1}. The dotted line is the shift in baseline determined from the nonlinear regression with respect to eq 1.

eq 1, it is possible to obtain estimates for T_d, $\Delta_dH(T_d)$, and Δ_dC_p. Close agreement between the calculated and the experimental profile has to be considered as a necessary and sufficient condition to conclude that the denaturation is a two-state N ⇔ D transition. We adopted this approach in analyzing 1000 data points for each measurement, by performing a nonlinear regression with respect to eq 1, using the Levenberg−Marquardt algorithm (*21*), as implemented in the Optimization Toolbox of MATLAB. The standard deviation of the calculated points from the experimental ones gives a measure of the adequacy of the fit in each case. It is defined as

$$\sigma = [\sum(\langle\Delta C_p(i)\rangle_{calc} - \langle\Delta C_p(i)\rangle_{exp})^2/n]^{1/2} \qquad (3)$$

where $\langle\Delta C_p(i)\rangle_{exp}$ is the ith value of the experimental excess heat capacity, $\langle\Delta C_p(i)\rangle_{calc}$ is the corresponding calculated value, and n is the total number of points considered in the analysis (1000 in our case).

Effect of DSC Data Truncation. We investigated the effect of observing an incomplete DSC peak and an undefined posttransition baseline on the accuracy of the thermodynamic parameters determined by the nonlinear regression procedure. The high-temperature side of the $\langle\Delta C_p\rangle$ profile at pH 2.5 of Sso7d was deliberately deleted with increasing severity, and the remaining data were subjected to nonlinear regression with respect to eq 1, to obtain estimates for T_d, $\Delta_dH(T_d)$, and Δ_dC_p. It is to be noted that in this manner we included the posttransition baseline in the nonlinear regression, assuming that its slope is equal to zero, and its y-intercept corresponds to Δ_dC_p. The $\langle\Delta C_p\rangle$ profile at pH 2.5 of Sso7d is shown in Figure 1, together with the shift in baseline resulting from the difference in heat capacity between the denatured and native states.

We verified on simulated two-state DSC curves that, by neglecting the posttransition baseline in the nonlinear regression procedure, the values of T_d and $\Delta_dH(T_d)$ determined are higher than the true values (data not shown). This should be particularly true in the case of the DSC profiles of Sso7d and its mutants, because the maximum height does not exceed 18 kJ mol^{-1}, while the value of Δ_dC_p is as high as 3.2 kJ K^{-1} mol^{-1}.

The results of our test, reported in Table 1, demonstrated that a reliable determination of T_d, $\Delta_dH(T_d)$, and Δ_dC_p is obtained with as little as 60% of the DSC peak data analyzed.

Table 1: Effect of DSC Data Truncation on the Values of Thermodynamic Parameters Obtained from the Nonlinear Regression[a]

cutoff temperature (°C)	T_d (°C)	$\Delta_dH(T_d)$ (kJ mol^{-1})	Δ_dC_p (kJ K^{-1} mol^{-1})	σ (J K^{-1} mol^{-1})
100	65.5	180.5	2.40	475
95	65.5	180.0	2.55	481
90	65.5	179.1	2.60	496
87	65.5	184.2	2.15	509
84	65.4	185.1	2.80	513
80	65.4	183.5	2.85	521
77	65.3	178.1	2.15	518
74	65.3	177.2	1.95	546
70	65.4	182.7	2.65	555

[a] The DSC data are those of Sso7d at pH 2.5, 10 mM glycine HCl buffer and 100 mM NaCl, as shown in Figure 1. σ is the standard deviation of the fit evaluated according to eq 3; see the text for further details.

The value of T_d varies by no more than 0.4 °C, that of $\Delta_dH(T_d)$ by no more than 5.0 kJ mol^{-1}, and that of Δ_dC_p by no more than 0.5 kJ K^{-1} mol^{-1}. Similar conclusions were reached by McCrary and colleagues in their detailed study of Sac7d (*22*). At first sight, this finding may be surprising, but it can be readly rationalized. According to eq 1, the height and the broadness of a perfect two-state DSC peak are determined by the values of T_d and $\Delta_dH(T_d)$; when T_d is kept fixed and $\Delta_dH(T_d)$ is increased, the height of the DSC peak increases, while its broadness decreases. Clearly, the height, but not the broadness, of the peak is also influenced by the value of Δ_dC_p. Therefore, only one set of the three parameters T_d, $\Delta_dH(T_d)$, and Δ_dC_p should be able to fit an experimental two-state DSC profile. We concluded that reliable thermodynamic parameters can be obtained from DSC scans in which incomplete DSC peaks are measured because of instrumental limitations. On the basis of these findings, we adopted the same procedure for analyzing all DSC profiles obtained over a broad range of pH for Sso7d and its three mutants, to determine consistent results among them.

RESULTS

All DSC measurements were performed in 10 mM buffer with 100 mM NaCl, using a scan rate of 1 K min^{-1}. Under these experimental conditions, the thermal denaturation of the proteins investigated proved to be reversible according to the reheating criterion; two successive scans of the same sample were almost superimposable. Therefore, it is legitimate to apply equilibrium thermodynamics in analyzing DSC data. The thermodynamic parameters calculated from the analysis of DSC profiles, at different pH values, for Sso7d and its three mutants are collected in Table 2.

For Sso7d, the values of both T_d and $\Delta_dH(T_d)$ progressively increase from 64.0 °C and 170 kJ mol^{-1} at pH 2.3 to 95.1 °C and 265 kJ mol^{-1} at pH 4.0. DSC experiments on Sso7d at pH >4.0 could not be carried out because of instrumental limitations. A linear regression of the $\Delta_dH(T_d)$ versus T_d plot has given a Δ_dC_p of 2.8 ± 0.2 kJ K^{-1} mol^{-1} (r = 0.99). It is worth noting that the values of T_d, $\Delta_dH(T_d)$, and Δ_dC_p can be superimposed with to those determined by Ladenstein and co-workers (*13*) for Sso7d in the same pH range. These authors used solutions containing 5 mM buffer, but we have verified that the values of T_d and $\Delta_dH(T_d)$ are not influenced

Table 2: Thermodynamic Parameters Of The Temperature-Induced Denaturation of Sso7d and Its Three Mutants, Obtained from DSC Scans, at Various pH Values[a]

	pH	T_d (°C)	$\Delta_dH(T_d)$ (kJ mol^{-1})	Δ_dC_p (kJ K^{-1} mol^{-1})	σ (J K^{-1} mol^{-1})
Sso7d	2.3	64.0	170	2.0	498
	2.5	65.5	180	2.4	475
	2.7	71.1	195	2.4	511
	2.8	74.0	205	1.9	565
	2.9	76.3	210	2.7	533
	3.0	78.8	215	3.1	595
	3.2	84.2	230	3.0	561
	3.6	90.3	245	2.5	547
	3.8	92.4	250	2.9	586
	4.0	95.1	265	2.3	591
F31A-Sso7d	3.0	53.0	135	1.9	487
	3.2	56.0	140	2.0	495
	3.5	60.5	150	2.2	504
	4.0	71.0	175	2.3	512
	4.5	73.0	180	3.0	546
	4.9	74.7	190	1.9	575
	5.0	74.3	185	2.0	583
	5.5	74.7	190	2.1	529
	5.6	74.5	185	1.9	603
	5.8	73.7	180	2.4	591
	6.0	75.1	190	2.0	515
	6.9	74.1	185	2.4	527
	7.2	73.9	180	2.1	573
F31Y-Sso7d	2.6	63.0	160	2.3	507
	3.0	74.2	185	2.8	488
	3.6	78.4	195	2.6	475
	3.8	80.1	200	1.9	518
	4.0	83.6	210	2.5	525
	4.2	84.8	210	3.0	547
	4.6	86.0	215	2.1	578
	4.9	88.0	225	2.0	591
	5.2	87.6	220	2.4	609
	5.5	88.5	230	2.8	541
	6.0	88.2	225	3.0	567
	6.5	88.0	220	2.7	509
	7.0	87.8	220	2.4	553
W23A-Sso7d	2.1	57.9	155	2.4	468
	2.5	61.8	165	2.0	485
	2.8	63.9	170	2.6	506
	3.0	67.1	175	1.9	511
	3.3	74.2	195	2.2	498
	3.5	79.3	210	3.1	521
	3.7	83.8	220	2.8	535
	3.8	87.2	230	2.7	549
	4.6	90.1	240	2.0	558
	5.0	91.6	245	3.2	607
	5.5	92.5	250	3.0	602
	6.0	92.3	245	2.5	583
	6.5	92.7	250	2.2	577
	7.0	92.1	245	2.7	546

[a] In all measurements, the buffer concentration was 10 mM with 100 mM NaCl. For each pH, we performed three independent DSC measurements. Each figure is the average of the values calculated by the nonlinear regression over the three DSC measurements; in addition, the values of $\Delta_dH(T_d)$ and Δ_dC_p have been rounded off to the nearest multiple of 5 and 10, respectively. The uncertainty in the T_d estimates does not exceed 0.3 °C, whereas the uncertainties in the estimates for $\Delta_dH(T_d)$ and Δ_dC_p amount to about 5 and 10%, respectively, of reported values. The values of σ, the standard deviation of the fit, are the highest ones obtained for each pH condition.

by ionic strength in the range of 0−200 mM NaCl (data not shown). Therefore, we used for Sso7d, at pH >4.0, the values of T_d and $\Delta_dH(T_d)$ determined by Ladenstein and co-workers (*13*). It proved that Sso7d has the maximal thermal stability in the pH range of 4.5−7.0 with a practically constant T_d of 98.2 ± 0.4 °C and a $\Delta_dH(T_d)$ of 267 ± 5 kJ mol^{-1}.

For F31A-Sso7d, the values of both T_d and $\Delta_dH(T_d)$ progressively increase from 53.0 °C and 135 kJ mol^{-1} at pH 3.0 to 74.7 °C and 190 kJ mol^{-1} at pH 4.9. On the other hand, in the pH range of 4.9−7.2 the thermal stability of F31A-Sso7d remains practically constant, with a T_d of 74.4 ± 0.5 °C and a $\Delta_dH(T_d)$ of of 186 ± 5 kJ mol^{-1}. The F31A substitution causes a very marked decrease of folded structure thermal stability; the value of T_d decreases by about 24 °C with respect to that of Sso7d. It is worth noting the dramatic effect that the substitution of a single residue has on the thermal stability of Sso7d. The $\Delta_dH(T_d)$ versus T_d plot is linear ($r = 0.99$), and $\Delta_dC_p = 2.5 \pm 0.2$ kJ K^{-1} mol^{-1}.

For F31Y-Sso7d, the values of both T_d and $\Delta_dH(T_d)$ strongly depend on pH in the range of 2.6−4.9: $T_d = 63.0$ °C and $\Delta_dH(T_d) = 160$ kJ mol^{-1} at pH 2.6, whereas $T_d = 88.0$ °C and $\Delta_dH(T_d) = 225$ kJ mol^{-1} at pH 4.9. On the contrary, in the pH range of 4.9−7.0, the thermal stability of F31Y-Sso7d remains practically constant, with a T_d of 88.0 ± 0.3 °C and a $\Delta_dH(T_d)$ of 223 ± 4 kJ mol^{-1}. The F31Y substitution, even though very conservative for the aromatic cluster, causes a marked decrease of folded structure thermal stability; the value of T_d decreases by about 10 °C with respect to that of Sso7d. A linear regression of the $\Delta_dH(T_d)$ versus T_d plot has given a Δ_dC_p of 2.6 ± 0.3 kJ K^{-1} mol^{-1} ($r = 0.98$).

For W23A-Sso7d, the values of both T_d and $\Delta_dH(T_d)$ progressively increase from 57.9 °C and 155 kJ mol^{-1} at pH 2.1 to 91.6 °C and 245 kJ mol^{-1} at pH 5.0, respectively. On the other hand, in the pH range of 5.0−7.0, the thermal stability of W23A-Sso7d remains practically constant, with T_d equal to 92.2 ± 0.4 °C and $\Delta_dH(T_d)$ equal to 247 ± 2 kJ mol^{-1}. The W23A substitution decreases the thermal stability of folded structure, even though the side chain of residue 23 is exposed to the solvent (*11, 12*); T_d is 6 °C lower than that of Sso7d. The $\Delta_dH(T_d)$ versus T_d plot proves to be linear ($r = 0.99$), and $\Delta_dC_p = 2.7 \pm 0.2$ kJ K^{-1} mol^{-1}. It is worth noting that the values of Δ_dC_p calculated from the slope of the $\Delta_dH(T_d)$ versus T_d plots for the four proteins are consistent with those obtained by performing a numerical average over the values determined for each scan.

DISCUSSION

According to CD, FTIR, and NMR spectra, the folded conformations of the three mutants proved to be very similar to that of Sso7d (*14*); this is an important point for a correct analysis of the effect of a given amino acid substitution on the protein thermal stability. First of all, it is worth noting that the T_d values of the three Sso7d mutants show a marked pH dependence up to pH around 5.0, and then practically level off, remaining constant up to pH 7.0. This behavior is consistent with that shown by Sso7d (*13*). As the three amino acid substitutions do not alter the content of ionizing groups in the protein and therefore its isoelectric point, they do not modify the pH dependence of protein thermal stability.

In addition, the values of Δ_dC_p, calculated for Sso7d and its three mutants from the $\Delta_dH(T_d)$ versus T_d plots, are very similar to each other and to that determined by Ladenstein and co-workers for Sso7d, 2.6 ± 0.3 kJ K^{-1} mol^{-1} (*13*). This finding is consistent with the expectation from the models

Table 3: Average Values of Thermodynamic Parameters for Sso7d and Its Three Mutants under Conditions of Maximal Thermal Stability[a]

protein	T_d (°C)	$\Delta_dH(T_d)$ (kJ mol^{-1})	$\Delta_dS(T_d)$ (J K^{-1} mol^{-1})	Δ_dH(98.2 °C) (kJ mol^{-1})	Δ_dS(98.2 °C) (J K^{-1} mol^{-1})	Δ_dC_p (kJ K^{-1} mol^{-1})
Sso7d	98.2 ± 0.4	267 ± 5	719 ± 14	267 ± 5	719 ± 14	2.6 ± 0.3
F31A	74.4 ± 0.5	186 ± 5	535 ± 15	246 ± 7	701 ± 20	2.5 ± 0.2
F31Y	88.0 ± 0.3	223 ± 4	618 ± 11	250 ± 5	691 ± 14	2.6 ± 0.3
W23A	92.2 ± 0.4	247 ± 2	676 ± 6	263 ± 3	720 ± 7	2.7 ± 0.2

[a] Values for Sso7d are numerical averages of the values determined by Ladenstein and co-workers for the pH range of 4.5−7.0 (seven figures from Table 3 of ref *13*). Values for the three mutants of Sso7d are numerical averages of the values reported in Table 2 of this study for the pH range of 4.9−7.2 (eight figures for F31A-Sso7d, six figures for F31Y−Sso7d, and five figures for W23A-Sso7d). Reported errors for T_d and $\Delta_dH(T_d)$ are the standard deviations of the normal distribution of the single figures at different pHs, assumed to be independent variables. Errors for $\Delta_dS(T_d)$, Δ_dH(98.2 °C), and Δ_dS(98.2 °C) are calculated by propagating the errors for $\Delta_dH(T_d)$ and T_d, using standard formulas (*31*). Errors in Δ_dC_p are the standard deviations of linear regressions for the $\Delta_dH(T_d)$ versus T_d plots.

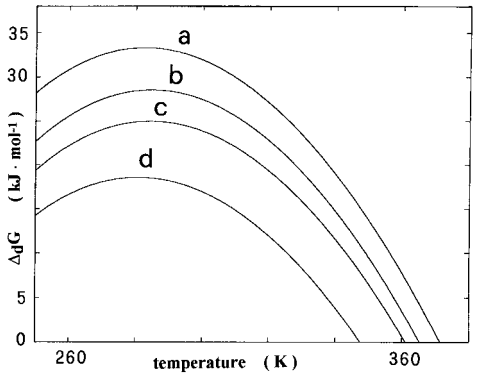

FIGURE 2: Comparison of the stability curves of Sso7d (curve a), W23A-Sso7d (curve b), F31Y-Sso7d (curve c), and F31A-Sso7d (curve d). They have been calculated with eq 4 using the values of thermodynamic parameters under conditions of maximal stability, reported in Table 3.

developed to calculate Δ_dC_p (*23*−*25*). In fact, the maximum variation in Δ_dC_p determined by the F31A substitution can be calculated by considering that the side chain of residue 31 is completely buried in the protein core, and that the difference in the nonpolar ASA between Phe and Ala amounts to about 100 Å^2 (*26*). Since each square angstrom of nonpolar ASA buried in the protein core contributes 2.0 J K^{-1} mol^{-1} Å^{-2} to Δ_dC_p (*27*), the decrease in Δ_dC_p should not exceed 200 J K^{-1} mol^{-1}, a figure below the limit of experimental uncertainty.

On the basis of such findings, we performed a comparison of the thermodynamic stability of Sso7d with that of its three mutants. The mean values of T_d, $\Delta_dH(T_d)$, $\Delta_dS(T_d)$, and Δ_dC_p in the pH range of 5.0−7.0 for the four proteins are shown in Table 3. These thermodynamic parameters allow the determination of the stability curves (*28*), Δ_dG versus T, of the four proteins, according to the equation

$$\Delta_dG(T) = \Delta_dH(T_d)[1 - (T/T_d)] + \Delta_dC_p[T - T_d - T\ln(T/T_d)] \quad (4)$$

which is correct assuming that Δ_dC_p is temperature-independent. This assumption is validated in this case by the finding that the $\Delta_dH(T_d)$ versus T_d plots proved to be linear over a wide temperature range, as already described by Ladenstein and co-workers (*13*). The calculated stability curves are shown in Figure 2. A comparison of them indicates that the amino acid substitutions do not practically affect the point of maximal stability, as it occurs always around 285 K. However, the corresponding values of Δ_dG are different: 33.7 kJ mol^{-1} for Sso7d, 28.5 kJ mol^{-1} for W23A-Sso7d, 24.5 kJ mol^{-1} for F31Y-Sso7d, and 18.6 kJ mol^{-1} for F31A-Sso7d. The maximum value of Δ_dG for Sso7d is comparable to those determined for mesophilic proteins (*24*), validating the suggestion by Jaenicke that the stability curves of thermophilic proteins are flattened with respect to those of mesophilic counterparts (*29*). In addition, Orban and co-workers (*30*) pointed out that high T_d values with normal thermodynamic stability at room temperature is a typical behavior of very small globular proteins because they tend to have relatively small values for $\Delta_dS(T_d)$ and Δ_dC_p per mole of protein, due to their small size.

To reach a deeper understanding of the molecular origin of such a difference in thermodynamic stability, we calculated the values of Δ_dH and Δ_dS at a common temperature for the four proteins, using the equations

$$\Delta_dH(T) = \Delta_dH(T_d) + \Delta_dC_p(T - T_d) \quad (5)$$

$$\Delta_dS(T) = [\Delta_dH(T_d)/T_d] + \Delta_dC_p\ln(T/T_d) \quad (6)$$

which are correct assuming that Δ_dC_p is temperature-independent. Comparison at any temperature would be theoretically valid, but we selected, as a reference, the denaturation temperature of Sso7d (T_d = 98.2 °C) to minimize the errors associated with the extrapolation procedure. In addition, since the values of Δ_dC_p are very similar for the four proteins, the differences in Δ_dH and Δ_dS depend very little on temperature. The values of Δ_dH(98.2 °C) and Δ_dS(98.2 °C) for Sso7d, F31A-Sso7d, F31Y-Sso7d, and W23A-Sso7d are shown in the fifth and sixth columns of Table 3, respectively. The F31A and F31Y substitutions affect only slightly the entropy change but cause a decrease in the average value of Δ_dH(98.2 °C) from 267 ± 5 to 246 ± 7 and 250 ± 5 kJ mol^{-1}, respectively. This suggests that the destabilization of folded structure has an enthalpic origin. The F31A substitution causes the loss of a significant amount of van der Waals interactions in the protein hydrophobic core, as the volume of the Phe side chain is much larger than that of the Ala side chain (129.7 versus 26.3 Å^3), according to the analysis of Chothia and co-workers (*32*). In addition, the partial destruction of the aromatic cluster of Phe5, Tyr7, Phe31, and Tyr33 should cause an enthalpic destabilization of native structure, as suggested by Burley and Petsko (*33*). The creation of a cavity with an only partial structural relaxation of surrounding groups is the most plausible explanation for the very marked decrease in thermal stability caused by the F31A substitution. In fact, molecular dynamics calculations determined that Phe31 has the largest van der Waals energy among all the amino acid residues of Sso7d

(*34*), because Phe31 is located in a strongly nonpolar region involving not only the already mentioned aromatic cluster but also the side chains of Val3, Val14, Ile19, Val22, Ile29, Val45, and Leu54. In all probability, the interactions among these side chains are so strong that a complete structural relaxation can be prevented, even in the absence of the Phe31 side chain.

In the case of the F31Y substitution, the enthalpic penalty associated with the dehydration and burial in the protein hydrophobic core of the hydroxyl group should be the origin of the destabilization (*35*). With the substitution of Phe31 with Tyr, the aromatic cluster should remain intact and no cavity should be created, as the side chain volume is 129.7 Å^3 for Phe and 133.3 Å^3 for Tyr (*32*). In all probability, the hydroxyl group buried in the protein core is not involved in a hydrogen bond, because the region is very rich in nonpolar moieties. The enthalpy loss due to the dehydration of the OH group, amplified by the hydrophobicity of the protein core and not counterbalanced by the gain for the formation of an intramolecular hydrogen bond, should cause the destabilization of the folded conformation (*35*, *36*). Such destabilization can be also explained on the basis of the difference in hydrophobicity between Phe and Tyr; $\Delta_{tr}G =$ 10.2 and 5.6 kJ mol^{-1} at 25 °C for Phe and Tyr, respectively, according to the *n*-octanol hydrophobicity scale of Fauchere and Pliska (*37*).

The W23A substitution, involving a residue whose side chain is exposed to the solvent, has no effect on the entropy change and causes a very slight decrease in the average value of $\Delta_d H$(98.2 °C) (263 ± 2 versus 267 ± 5 kJ mol^{-1}). The large aromatic side chain of Trp should interact more favorably with water than the small aliphatic side chain of Ala, through the formation of hydrogen bonds involving the delocalized π electrons of the ring (*38*, *39*). In addition, molecular dynamics calculations (*34*) showed that the large side chain of Trp23 is involved in favorable van der Waals interactions with other groups of the protein that the small side chain of Ala would not be able to maintain.

In conclusion, DSC data reveal that the hydrophobic core, mainly constituted by the aromatic cluster of Phe5, Tyr7, Phe31, and Tyr33 with herringbone geometry, plays a major role in determining the stability of Sso7d, even though other factors are important, as indicated by the destabilization caused by the W23A substitution.

ACKNOWLEDGMENT

We thank Dr. B. K. Lee for a critical reading of an earlier version of the manuscript. The comments by referees were also invaluable in shaping the final form of the paper.

REFERENCES

1. Anfinsen, C. B. (1973) *Science 181*, 223−230.
2. Privalov, P. L. (1979) *Adv. Protein Chem. 33*, 167−241.
3. Stetter, K. O., Fiala, G., Huber, G., Huber, R., and Segerer, A. (1990) *FEMS Microbiol. Rev. 75*, 117−124.
4. Jaenicke, R., Schurig, H., Beaucamp, N., and Ostendorp, R. (1996) *Adv. Protein Chem. 48*, 181−269.
5. Choli, T., Henning, P., Wittmann-Liebold, B., and Reinhard, R. (1988) *Biochim. Biophys. Acta 950*, 193−203.
6. Fusi, P., Tedeschi, G., Aliverti, A., Ronchi, S., Tortora, P., and Guerritore, A. (1993) *Eur. J. Biochem. 211*, 305−310.
7. De Rosa, M., Gambacorta, A., Nicolaus, B., Giardina, P., Poerio, E., and Buonocore, V. (1984) *Biochem. J. 224*, 407−414.
8. Fusi, P., Grisa, M., Mombelli, E., Consonni, R., Tortora, P., and Vanoni, M. (1995) *Gene 154*, 97−102.
9. Baumann, H., Knapp, S., Karshikoff, A., Ladenstein, R., and Hard, T. (1995) *J. Mol. Biol. 247*, 840−846.
10. Lundback, T., and Hard, T. (1996) *J. Phys. Chem. 100*, 17690−17695.
11. Baumann, H., Knapp, S., Lundback, T., Ladenstein, R., and Hard, T. (1994) *Nat. Struct. Biol. 1*, 808−819.
12. Consonni, R., Limiroli, R., Molinari, H., Fusi, P., Grisa, M., Vanoni, M., and Tortora, P. (1995) *FEBS Lett. 372*, 135−139.
13. Knapp, S., Karshikoff, A., Berndt, K. D., Christova, P., Atanasov, B., and Ladenstein, R. (1996) *J. Mol. Biol. 264*, 1132−1144.
14. Fusi, P., Goossens, K., Consonni, R., Grisa, M., Puricelli, P., Vecchio, G., Vanoni, M., Zetta, L., Heremans, K., and Tortora, P. (1997) *Proteins 29*, 381−390.
15. Gill, S. C., and von Hippel, P. H. (1989) *Anal. Biochem. 182*, 319−326.
16. Izatt, R. M., and Christensen, J. J. (1976) in *The CRC Handbook of Biochemistry and Molecular Biology, Physical and Chemical Data* (Fasman, G. D., Ed.) 3rd ed., Vol. 1, pp 151−360, CRC Press, Boca Raton, FL.
17. Barone, G., Del Vecchio, P., Fessas, D., Giancola, C., and Graziano, G. (1992) *J. Therm. Anal. 38*, 2779−2790.
18. Freire, E., and Biltonen, R. L. (1978) *Biopolymers 17*, 463−479.
19. Freire, E. (1994) *Methods Enzymol. 240*, 502−530.
20. Straume, M., and Freire, E. (1992) *Anal. Biochem. 203*, 259−268.
21. Marquardt, D. (1963) *J. Appl. Math. 11*, 431−441.
22. McCrary, B. S., Edmondson, S. P., and Shriver, J. W. (1996) *J. Mol. Biol. 264*, 784−805.
23. Murphy, K. P., and Freire, E. (1992) *Adv. Protein Chem. 43*, 313−361.
24. Makhatadze, G. I., and Privalov, P. L. (1995) *Adv. Protein Chem. 47*, 307−425.
25. Graziano, G., Catanzano, F., Del Vecchio, P., Giancola, C., and Barone, G. (1996) *Gazz. Chim. Ital. 126*, 559−567.
26. Livingstone, J. R., Spolar, R. S., and Record, M. T. (1991) *Biochemistry 30*, 4237−4244.
27. Graziano, G., and Barone, G. (1996) *J. Am. Chem. Soc. 118*, 1831−1835.
28. Becktel, W. J., and Schellman, J. A. (1987) *Biopolymers 26*, 1862−1877.
29. Jaenicke, R. (1991) *Eur. J. Biochem. 202*, 715−728.
30. Alexander, P., Fahnestock, S., Lee, T., Orban, J., and Bryan, P. (1992) *Biochemistry 31*, 3597−3603.
31. Bevington, P. R., and Robinson, D. K. (1992) *Data Reduction and Error Analysis for the Physical Sciences*, McGraw-Hill, New York.
32. Harpaz, Y., Gerstein, M., and Chothia, C. (1994) *Structure 2*, 641−649.
33. Burley, S. K., and Petsko, G. A. (1985) *Science 229*, 23−28.
34. Mombelli, E., Afshar, M., Fusi, P., Mariani, M., Tortora, P., Connelly, J. P., and Lange, R. (1997) *Biochemistry 36*, 8733−8742.
35. Yang, A. S., Sharp, K. A., and Honig, B. (1992) *J. Mol. Biol. 227*, 889−900.
36. Honig, B., and Yang, A. S. (1995) *Adv. Protein Chem. 46*, 27−58.
37. Fauchere, J. L., and Pliska, V. E. (1983) *Eur. J. Med. Chem. 18*, 369−375.
38. Linse, P. (1990) *J. Am. Chem. Soc. 112*, 1744−1750.
39. Makhatadze, G. I., and Privalov, P. L. (1994) *Biophys. Chem. 50*, 285−291.

BI972994K